

METHANATION FOR COAL HYDROGASIFICATION

A. L. Lee, H. L. Feldkirchner and D. G. Tajbl*

Institute of Gas Technology
Chicago, Illinois 60616

INTRODUCTION

The goals of this study are as follows:

- Test commercial methanation catalysts to determine the most suitable one for the methanation step of the IGT HYGAS Process for producing pipeline gas from coal.
- Perform a life study on the chosen catalyst.
- Obtain pilot plant design data for anticipated gas compositions from the hydrogasification reactor.
- Develop a kinetic equation for the methanation catalyst selected under actual operating conditions.

Dirksen and Linden⁴ did extensive work on synthesis-gas methanation and gave detailed discussions of their work. Tajbl et al.¹⁰ presented the results of the commercial catalyst selection for the HYGAS Process and described the experimental apparatus. Earlier we obtained a rate expression⁶ for the design of the pilot plant reactor and developed a practical reactor operating scheme.

This paper presents the results of the catalyst life study, a reactor stability study, and a kinetic study. In addition to the references cited in the text, we have also presented a literature survey. For a more complete review of literature prior to 1963, refer to the bulletin by Dirksen and Linden.⁴

KINETIC STUDY

The apparatus used for this study was described in detail previously.¹¹ A schematic diagram of the modified system is presented in Figure 1. The modifications are the benzene saturator, high-pressure sampling, and a better gas chromatograph. The purpose of a benzene saturator is to study the effect of traces of benzene in the feed gas on the rate of methanation and the long-term activity of the catalyst. Benzene is produced in the HYGAS Process for use in the slurry feeding of coal to the gasifier. Thus, traces of benzene will be present in the methanator feed stream.

To obtain pilot plant design data, three feed gases covering the range of anticipated methanation feed compositions were used (Table I). The results were presented elsewhere.¹¹ To summarize these findings, we found that a rate expression⁶ (Equation 1) represents the data:

$$r = k p_{\text{CO}}^{0.62} \quad (1)$$

* Now with Mobil Oil Corporation, Paulsboro, New Jersey.

Table 1. COMPOSITIONS OF FEED GASES

Feed	High CO	Intermediate CO	Low CO
	mole %		
Carbon Monoxide	10.0	7.0	2.4
Carbon Dioxide	2.1	2.1	2.0
Hydrogen	34.5	26.1	13.5
Methane	53.4	64.8	82.1
Total	100.0	100.0	100.0

Using the same data, Wen *et al.*¹³ found a rate equation:

$$r = k p_{\text{CO}}^{0.7} p_{\text{H}_2}^{0.3} \quad (2)$$

Both equations of the form of 1 and 2 can fit the data reasonably well, as Weller¹¹ has shown.

To improve the above rate expressions for the IGT methanation process, the reaction-rate study was extended, mainly in tests on 1/4-inch catalyst pellets that will be used in our plant. Feed gases containing only H₂ and CO were used to determine the CO order; feed gases containing H₂, CO, and He were used to determine the H₂ order and the effect of an inert on the methanation rate; feed gases containing H₂, CO, and CH₄ were used to determine the effect of a large CH₄ concentration in the feed on the rate of methanation and hence on the CH₄ order; feed gases containing H₂, CO, CH₄, and C₆H₆ were used to determine the effect of benzene; and feed gases of H₂, CO, CH₄, and C₆H₆ with traces of mercaptan (0.3 ppm) and thiophene (0.8 ppm) were used to determine the effect of organic sulfur on the activity of the catalyst. These data are presented in Table 2.

We found that the H₂ order is about 0.5, with and without CH₄ in the feed gas, as illustrated in Figure 2; the effect of CH₄ is noticeable only at near-equilibrium conditions (Figure 2); the order of CO is about 1 (Figure 3); the effect of He is nil; the effect of C₆H₆ (up to 1% in feed) is nil; and the effect of organic sulfur in the gas on the rate of the methanation reaction is nil at the low concentration levels studied (mercaptans and thiophene up to 1.1 ppm).

The rate expression:

$$r = k p_{\text{CO}} p_{\text{H}_2}^{0.5} \quad (3)$$

correlates most of the experimental data except when excess H₂ and/or CH₄ are present. To cover the entire range of gas compositions, Equation 3 was modified to the following form:

$$r = \frac{k p_{\text{CO}} p_{\text{H}_2}^{0.5}}{1 + K_2 p_{\text{H}_2} + K_3 p_{\text{CH}_4}} \quad (4)$$

The results are presented in Table 2 and Figure 4.

There are numerous rate expressions proposed for methanation in the literature. Some of those that are related to this study are presented in Table 3. Most of the work in the literature was done with feed gases containing H₂ and CO or H₂, CO, and CO₂ only and at relatively low pressures. Table 3 is presented to give a quick over-all view of the various methanation rate equations proposed.

Table 3. RATE EQUATIONS FOR METHANATION PROPOSED BY VARIOUS INVESTIGATORS

Author(s)	Rate Equation	Temperature, Pressure	Remarks
Nicola et al. ⁸	$r = k \frac{P_{H_2}^{0.7} P_{CO}}{P_{CO_2}}$	250-300°C, 0.1-1.0 atm	This work is concentrated on CO ₂ hydrogenation on a nickel catalyst. Very little work is done on CO methanation.
Akers and White ¹	$r = \frac{K_1 P_{CO} P_{H_2}}{K_2 + P_{CO} + P_{CO_2} + P_{CH_4} + P_{H_2O}}$	300-350°C, 1 atm	A reduced nickel catalyst was used. The water-gas shift reaction was also studied and a rate equation for the formation of CO ₂ was discussed.
Purley et al. ⁹	$r = \frac{1.1 P_{CO} P_{H_2}^{0.5}}{1 + 1.5 P_{H_2}}$	500-700°F, 14.7-400 psia	A nickel catalyst was used to study the initial rate of the CO-H ₂ reaction. This equation was derived by using sulfur-free mixtures of CO and H ₂ containing less than 30 mole % CO.
McKee ⁷	$r = k \frac{P_{H_2}^{0.5} P_{CO}}{P_{CO_2}}$	220°C, 21.4 atm	Platinum group metals were used as catalysts for the reaction: ZCO + 2H ₂ ⇌ CH ₄ + CO ₂ .
Barkley et al. ²	$r = \frac{k P_{CO} P_{H_2} - \frac{P_{CO} P_{H_2O}}{K}}{1 + K_1 P_{CO} + K_2 P_{CO_2}}$	1000°F	A study of the gas-phase reaction CO ₂ + H ₂ ⇌ CO + H ₂ O over an iron-copper catalyst. A mechanism for this reaction was postulated.
Bunder and White ³	$r = \frac{C_1 \left(P_{CO_2} P_{H_2} - \frac{P_{CH_4} P_{H_2O}}{K_1} \right)}{P_{H_2}^{0.5} + C_2 P_{CO_2} + C_3}$	500-750°F, 1 atm	A reduced nickel catalyst was used.
and	$r = \frac{C_1 \left(P_{CO_2} P_{H_2} - \frac{P_{CH_4} P_{H_2O}}{K_1} \right)}{P_{H_2}^{0.5} + C_2 P_{CO_2} + C_3}$		
Weller ¹²	$r = k P_{CO} P_{H_2}^{0.5}$		
Schoubye ¹⁰	$r = \frac{Z_1 \exp \left[-\frac{E_1}{RT} \right] P_{H_2}^n}{1 + Z_2 \exp \left[\frac{16650}{RT} \right] \left(\frac{P_{CO}}{P_{H_2}} \right)^{0.75}}$	200-300°C, 2-15 atm	Used Akers and White's data ¹ and arrived at this simpler rate expression which correlates rate data with about the same accuracy. Excellent discussion on the analysis of data. Nickel catalysts were used. Order of CO was found to be from 0 to -0.5.
Wan et al. ¹¹	$r = k P_{CO} P_{H_2}^{0.5}$	550-850°F, 14.7-1000 psia	IGT data were used in this analysis.
Tajiri ¹¹	$r = 7.85 \times 10^5 \exp \left[-\frac{17200}{RT} \right] \times CO$	550-600°F, 69 atm	Initial analysis of effluent gas mixture from hydrogasifier.
Lee ⁵	$r = k P_{CO} P_{H_2}^{0.5}$	550-850°F, 14.7-1000 psia	Analysis of feed gas mixtures of H ₂ -CO; H ₂ -CO-H ₂ ; H ₂ -CO-CH ₄ ; and H ₂ -CO-CH ₄ -CO ₂ -C ₂ H ₆ .
This study	$r = \frac{k_1 P_{CO} P_{H_2}^{0.5}}{1 + k_2 P_{H_2} + k_3 P_{CH_4}}$	550-850°F, 14.7-1000 psia	

CATALYST LIFE TESTS

When this program was begun, no successful work had been reported on fixed-bed methanation of high carbon monoxide, high-methane-content gases with typical commercial nickel catalysts. Thermodynamic calculations indicated that the gases that would have to be methanated would be capable of depositing carbon in the range of temperatures and pressures expected. Further, in packed-bed reactors, the high heat of reaction was expected to cause catalyst deactivation through hot spots and carbon deposition. These problems had been encountered by others.

We, therefore, set up a small laboratory test unit to test commercial catalysts in a fixed-bed reactor under the expected operating conditions. A schematic diagram of the unit is given in Figure 5. Synthetic gas mixtures were prepared having the following typical composition ranges.

<u>Component</u>	<u>Composition, mole %</u>
CO	3.5-12.7
CO ₂	0.6-3.2
H ₂	18.8-57.5
CH ₄	24.3-72.6
C ₂ H ₆	0.1-1.3
N ₂	1.2-4.0

Sulfur was removed from the feed gas to less than 0.1 ppm by beds of activated carbon and zinc oxide.

The unit was designed for around-the-clock operation with a minimum of operator attention. The feed gas rate, the reactor and guard chamber temperatures, and the unit pressure were controlled and recorded. The condensed product water was drained from the unit automatically by a liquid-level controller. The product-gas CO content was monitored by an MSA Lira model infrared analyzer and recorded continuously. Exit-gas volumes were recorded manually at regular intervals, and samples of feed and exit gases were taken throughout the test periods for analysis by gas chromatography.

A diagram of the reactor and electric heater and furnace is given in Figure 6. The 4-inch-deep catalyst bed was held between two packed beds of glass beads. The upper part of the reactor was enclosed in an electric furnace and the lower part was wrapped by an electric resistance heater. Bed temperatures were recorded at the four points indicated.

Initial tests were with a commercial nickel-on-alumina catalyst. The catalyst, supplied as 1/4-inch pellets, was crushed to -12+18 USS. Feed gases contained 4 mole percent CO in some tests and 13 mole percent in others. In all tests with this catalyst there was considerable carbon deposition. Higher temperatures were required to obtain sufficient catalyst activity for the desired reduction of carbon monoxide to 0.1 mole percent, which may have accelerated carbon deposition rates.

Tests with 1/8-inch pellets of nickel-on-kieselguhr catalyst were successful. One run lasted 1420 hours, during which time conditions were varied considerably (Table 4). Space velocities of over 9000 SCF/CF cat.-hr were used. The run was terminated voluntarily with the CO content of the exit gas still at only 0.1 mole percent. The CO₂ conversion showed no consistent trend with variations in operating conditions. Ethane hydrogenolysis was nearly complete for the entire run.

Table 4. LIFE TEST RESULTS

Run No.	Catalyst		LT-11		Nickel on Kieselguhr		0.00352		1152		1320		1420					
	19	80	217	288	421	464	558	653	771	820	820	986	1109	1152	1250	1320	1391	1420
1000	1005	1003	1000	1006	1006	1000	1000	1003	998	1014	1005	1006	1003	1000	1006	1006	1000	1010
Test Duration, hr																		
Temperature, °F																		
Preheater (1)																		
1-1/2 in. From Top (2)																		
4 in. From Top (3)																		
Product Gas (4)																		
Furnace																		
Feed Gas Composition (Dry), mole %																		
CO	4.3	4.0	3.5	3.5	4.0	4.0	4.0	3.7	3.7	3.8	4.2	3.7	3.7	3.7	3.7	3.7	3.7	3.7
CO ₂	1.5	1.4	1.0	0.8	0.8	0.8	0.7	0.7	0.7	0.6	0.6	0.8	0.8	0.8	0.8	0.8	0.8	0.8
H ₂	18.8	19.4	18.8	20.1	20.1	20.1	21.3	21.3	19.8	19.8	20.0	18.9	18.9	18.9	19.6	19.6	19.6	19.6
CH ₄	70.1	69.3	70.0	69.0	69.0	69.0	68.0	68.0	71.9	72.2	72.2	72.6	72.6	72.6	71.7	71.7	71.7	71.7
C ₂ H ₆	2.7	2.7	3.4	3.7	3.7	3.7	3.7	3.7	1.2	1.1	0.9	0.9	0.9	0.9	0.9	0.9	0.9	0.9
N ₂	2.6	3.2	3.3	3.3	2.4	2.4	6.0	6.0	2.7	1.9	3.1	3.1	3.1	3.1	3.1	3.1	3.1	3.1
Total	100.0	100.0	100.0	100.0	100.0	100.0	100.0	100.0	100.0	100.0	100.0	100.0	100.0	100.0	100.0	100.0	100.0	100.0
Space Velocity, SCF/cu ft-hr	2539	2590	2599	2596	2619	2619	4798	2619	4803	4803	5284	4832	4832	6852	4193	8664	4383	9130
Feed Rate, SCF/hr	8.99	9.12	9.15	9.14	9.22	16.56	8.34	16.89	9.24	16.91	18.60	17.01	24.12	14.76	30.50	15.43	32.14	
Product Gas Composition (Dry), mole %																		
CO	0.2	0.1	0.2	0.1	0.1	0.0	0.1	0.1	0.1	0.1	0.1	0.0	0.1	0.1	0.1	0.1	0.1	0.1
CO ₂	0.9	1.0	1.0	0.8	0.6	0.1	0.2	0.1	0.1	0.0	0.0	0.0	0.1	0.1	0.1	0.3	0.2	0.5
H ₂	1.8	1.8	1.7	1.4	1.5	1.6	1.5	2.1	3.3	2.8	4.2	3.0	3.3	3.3	2.6	3.3	2.9	4.0
CH ₄	93.6	93.5	93.6	94.4	94.2	94.9	95.0	94.3	92.9	93.9	92.5	93.3	92.9	93.4	93.4	92.6	93.3	91.5
C ₂ H ₆	0.2	0.1	0.2	0.2	0.2	0.1	0.1	0.1	0.4	0.0	0.0	0.0	0.0	0.0	0.1	0.0	0.0	0.0
N ₂	3.3	3.5	3.3	3.1	3.4	3.3	3.1	3.3	3.2	3.2	3.2	3.6	3.6	3.6	3.7	3.7	4.0	3.9
Total	100.0	100.0	100.0	100.0	100.0	100.0	100.0	100.0	100.0	100.0	100.0	100.0	100.0	100.0	100.0	100.0	100.0	100.0
Product, SCF/SCF feed	0.77	0.77	0.77	0.78	0.78	0.82	0.64	0.80	0.88	0.86	0.84	0.82	0.82	0.82	0.82	0.80	0.83	0.80
Heating Value, Btu/SCF	942	940	941	948	950	955	957	947	949	952	940	949	944	944	941	932	938	922
Carbon Recovery, %	91	92	93	93	92	96	77	97	104	103	99	98	98	98	99	96	100	94
Hydrogen Recovery, %	91	92	91	92	91	92	96	94	103	102	98	97	97	97	97	94	98	93
Oxygen Recovery, %	95	98	102	91	110	101	106	115	106	106	79	85	91	67	82	65	90	90
Total Material Recovery, %	92	92	92	91	94	97	77	98	104	103	99	97	97	97	97	95	98	94
Water Collected by Condensate																		
Measurement, g/hr	10.40	9.88	10.37	7.26	10.24	19.62	8.34	19.00	11.15	18.96	16.80	15.98	23.69	11.67	26.89	10.97	29.47	
CO Conversion, %	96	96	96	98	98	100	98	98	98	97	98	100	98	98	98	98	98	98
CO ₂ Conversion, %	53	44	44	37	41	90	84	89	87	100	100	100	90	90	92	76	81	60
C ₂ H ₆ Conversion, %	94	97	94	95	96	98	98	98	90	100	100	100	100	100	90	100	100	100

Although the nickel-on-kieselguhr catalyst is less strong than the nickel-on-alumina one, its superior performance makes it the preferred catalyst for the HYGAS Process.

REACTOR STABILITY

Because the methanation reaction is highly exothermic, it is conceivable that the catalyst-bed temperature could exceed the calculated adiabatic equilibrium temperature at some operating conditions and in some reactor configurations. Preliminary calculations indicated possible instability in the packed-bed methanation reactors for the HYGAS pilot plant and large-scale plants being designed. Therefore, a more detailed study of reactor stability was undertaken.

The first approach was an attempt to test for stability without requiring the solution of the several partial differential equations involved. One can reason that in an adiabatic steady-state system with the single-path catalytic reaction presumed here, the temperature of the gas phase must lie between the initial and final equilibrium temperatures. The difference between the catalyst and gas-phase temperature is proportional to the reaction rate if the gas-particle heat transfer coefficient is assumed constant. Therefore, if the catalyst temperature is not excessive at the known inlet conditions, a sufficient condition for the system to be stable is that the reaction rate decreases with distance through the reactor; that is, a sufficient condition for stability is -

$$\frac{dr}{dz} < 0 \quad (5)$$

But in this system the reactant CO decreases with distance so that the condition is equivalent to:

$$\frac{dr}{d(X_{CO})_g} > 0 \quad (6)$$

where the reaction rate is a function of the catalyst temperature, and the concentration of CO near the surface is in turn dependent on the CO concentration in the gas phase. Equation 7 follows directly from Equation 6:

$$\left(\frac{\partial r}{\partial (X_{CO})_s} \right)_{T_s} \frac{d(X_{CO})_s}{d(X_{CO})_g} + \left(\frac{\partial r}{\partial T_s} \right) (X_{CO})_s \frac{dT_s}{d(X_{CO})_g} = \frac{dr}{d(X_{CO})_g} > 0 \quad (7)$$

From steady-state considerations and neglecting the second-order effects of variation in physical properties with temperature and composition, one can show that -

$$T_s = \frac{r \cdot \Delta H}{h_t} + \left[\frac{(X_{CO})_o - (X_{CO})_g}{c_g} \right] (\Delta H + T_o) \quad (8)$$

$$(X_{CO})_s = (X_{CO})_g - \frac{r}{\rho_g h_m} \quad (9)$$

Operating on these equations leads to:

$$\frac{dr}{d(X_{CO})_g} = \frac{\left[\partial r / \partial (X_{CO})_s \right] - \Delta H / c_g \left[\partial r / \partial T_s \right]}{1 + \left[1 / h_m \rho_g \right] \left[\partial r / \partial (X_{CO})_s \right] - \Delta H / h_t \left[\partial r / \partial T_s \right]} \quad (10)$$

The right-hand side of Equation 10 requires the kinetics of the reaction in terms of the catalyst conditions. This is the case at hand. Noting that this quantity is greater than zero if the reaction rate is temperature-independent, one can conclude that for the kinetics proposed by Wen¹³ the system is always stable. Wen's interpretation of IGT data is that there is no temperature effect above 600 °F. However, our kinetic data retain a significant temperature dependence at high temperatures, which leads to negative values for the expression in Equation 10 with h_t and h_m appropriate to the expected flow regime.

A positive value of Equation 10 is sufficient for stability but not necessary. Consequently, negative values leave us in an indeterminate position. But we can, and did, calculate the values of T_s for the possible range of values of $\{X_{CO}\}_g$ from Equations 8 and 9. At the expected levels of transfer rates, with our kinetics, the computed catalyst temperature never exceeds the final temperature.

In Figure 7 the estimated catalyst temperatures are shown as a function of degree of conversion at the expected transfer rates (30,000 Btu/hr-sq ft per cu ft of void volume) for a 540 °F feed gas containing 4 mole percent CO in excess H_2 . Figure 7 also shows results for transfer rates that are reduced 30-fold (the heat and mass transfer coefficients proportionately) — an effect corresponding to a meaningless 900-fold decrease in velocity. The higher temperature levels only exceed the final temperature by 25 °F. Therefore, even spots in the reactor where the velocity is unusually low still would not become excessively hot.

The kinetics and the mass and heat transfer rates collected by IGT were used to estimate the required space velocities for the methanation process. In Figure 8, the results are given for a 4 mole percent CO feed gas at a 550 °F feed temperature in a steady-state system, with a feed rate of 126 lb-mole/hr-sq ft of reactor cross section. For a product gas with 0.1 mole percent CO, the space velocity is computed to be 47,000 SCF/CF-hr. A ninefold change in velocity affects the required space velocity by only 8%.

As a check, the system was calculated using kinetics proposed by Wen,¹³ which, because of the assumption of temperature independence above 600 °F, do not predict as high a reaction rate at the higher temperature as do our kinetics. The results are also given in Figure 8. Wen's kinetics lead to an estimate of space velocity to produce 0.1 mole percent CO at 550 °F with a space velocity of 27,000 SCF/CF-hr. Since it is quite probable that Wen interprets a diffusion limitation in the original experiments as a slow reaction rate, the 27,000 represents a lower bound on estimates of space velocities based on our original data. Our pilot plant methanation reactors were designed using a space velocity of less than 5000 SCF/CF-hr. It is possible that we can methanate the entire pilot plant output in two methanation stages.

ACKNOWLEDGMENT

This work is sponsored by the American Gas Association, Research and Development, and the U. S. Department of the Interior, Office of Coal Research. Their support is gratefully acknowledged. The advice and contributions of F. C. Schora, B. S. Lee, S. A. Weil, R. Noresco, and A. Talwalker are appreciated.

NOMENCLATURE

A	= surface equilibrium constant ¹
B	= surface equilibrium constant ¹
c	= heat capacity
C ₁	= reaction rate constant ³
C ₂	= surface equilibrium constant ³
C ₃	= surface equilibrium constant ³
C ₁ '	= reaction rate constant ³
C ₂ '	= surface equilibrium constant ³
C ₃ '	= surface equilibrium constant ³
D	= surface equilibrium constant ¹
E	= surface equilibrium constant ¹
E ₁	= activation energy ¹⁰
h _t	= heat transfer coefficient
h _m	= mass transfer coefficient
ΔH	= heat released per unit reaction
k	= reaction rate constant
K	= surface equilibrium constant
n	= order of reaction
p	= partial pressure
r	= reaction rate
r ₀	= initial reaction rate
R	= gas constant
T	= temperature
X	= mole fraction
Z	= distance through reactor
Z ₁	= Arrhenius constant ¹⁰
Z ₂	= constant ¹⁰

Greek Letter

ρ = density

Subscripts

g = gas

o = initial

s = surface

REFERENCES CITED

1. Akers, W. W. and White, R. R., "Kinetics of Methane Synthesis," Chem. Eng. Progr. 44, 553-66 (1948).
2. Barkley, L. W. et al., "Catalytic Reverse Shift Reaction," I&EC 44, 1066-71 (1952).
3. Binder, G. G. and White, R. R., "Synthesis of Methane From Carbon Dioxide and Hydrogen," Chem. Eng. Progr. 46, 563-74 (1950).
4. Dirksen, H. A. and Linden, H. R., "Pipeline Gas From Coal by Methanation of Synthesis Gas," IGT Res. Bull. No. 31. Chicago, July 1963.
5. Institute of Gas Technology, "Pipeline Gas From Coal - Hydrogenation," A.G.A. Project IU-4-1 and OCR Contract No. 14-01-0001-381 (1). Chicago, November 1969.
6. Institute of Gas Technology, "Pipeline Gas From Coal - Hydrogenation," A.G.A. Project IU-4-1 and OCR Contract No. 14-01-0001-381 (1). Chicago, September 1968.
7. McKee, D. W., "Interaction of H₂ and CO on Platinum Group Metals," J. Catal. 8, 240-49 (1967).
8. Nicolai, J., D'hont, M. and Jungers, J. C., "The Synthesis of Methane From Carbon Monoxide and Hydrogen on Nickel," Bull. Soc. Chim. Belgium 55, 160-76 (1946).
9. Pursley, J. A., White, R. R. and Sliepcevich, C., "The Rate of Formation of Methane From CO and H₂ With a Nickel Catalyst at Elevated Pressures," Chem. Eng. Progr. Sym. Ser. 4, 51-58 (1952).
10. Schoubye, P., "Methanation of CO on Some Ni Catalysts," J. Catal. 14, 238-46 (1969).
11. Tajbl, D. G., Feldkirchner, H. L. and Lee, A. L., "Cleanup Methanation for the Hydrogasification Process," ACS Div. Fuel Chem. Prepr. No. 4, 235-45 (1966) September; also in Advances in Chemistry Series No. 69, 166-79. Washington, D.C.: American Chemical Society, 1967.
12. Weller, S., "Analysis of Kinetic Data for Heterogeneous Reactions," A.I.Ch.E. J. 2, 59-62 (1956).
13. Wen, C. Y. et al., "Optimization of Fixed Bed Methanation Processes." Paper presented at the ACS Meeting, Atlantic City, New Jersey, September 1968.

LITERATURE SURVEY

1. Andrew, S.P.S., "Catalysts and Catalytic Processes in the Steam Reforming of Naphtha," I&EC Prod. Res. Develop. 8, 321-24 (1969).
2. Bienstock, D. et al., "Synthesis of High Btu Gas From CO and H₂ Using a Hot Gas Recycle Reactor," Paper No. CEP-60-14 in Proceedings of American Gas Association Operating Section. New York, 1960.
3. Boudart, M., "Kinetics on Ideal and Real Surfaces," A.I.Ch.E. J. 2, 62-64 (1956).
4. Carberry, J. J., "Designing Laboratory Catalytic Reactors," I&EC 56, 39-46 (1966).
5. Carberry, J. J., "Transport Phenomena and Heterogeneous Catalysis," Chem. Process Eng. 306-15 (1963) June.
6. Demeter, J. J., Haynes, W. P. and Youngblood, A. J., "Experiments With a Self-Generated Carbon-Expanded Iron Catalyst for Synthesis of Methane," Report No. 6425. Washington, D.C.: U.S. Dept. Interior, Bureau of Mines, 1963.
7. Dent, F. J. and Hebben, D., "The Catalytic Synthesis of Methane as a Method of Enrichment in Town Gas Manufacture," Gas Research Board Communication GRB 51. London, 1949.
8. Dent, F. J. et al., "An Investigation Into the Catalytic Synthesis of Methane for Town Gas Manufacture," Gas Research Board Communication GRB 20. London, 1945.
9. Feldkirchner, H. L. and Kniebes, D. V., "Effect of Nuclear Irradiation on the Activity of Iron Methanation Catalysts." Paper presented at ACS Meeting, Washington, D.C., March 20-24, 1962.
10. Field, J. H. et al., "Development of Catalysts and Reactor Systems for Methanation," I&EC Prod. Res. Develop. 3, 150-53 (1964).
11. Goldberger, W. M. and Othmer, D. F., "The Kinetics of Nickel Carbonyl Formation," I&EC Process Design Develop. 2, 202-09 (1963).
12. Greyson, M., "Methanation," in Catalysis, Vol. IV, Emmet, P. H., Ed., 473-511. New York: Reinhold, 1956.
13. Greyson, M. et al., "Synthesis of Methane," Report No. 5137. Washington, D.C.: U.S. Dept. Interior, Bureau of Mines, 1955.
14. Linden, H. R., "Conversion of Solid Fossil Fuels to High-Btu Pipeline Gas." Paper presented at A.I.Ch.E. Meeting, Denver, August 26-29, 1962.
15. Meller, A., "Catalytic Hydrogenation of CO - Methane Synthesis From Water Gas." Aust. Chem. Inst. J. Proc. 10, 100-14, 123-29 (1943).
16. Schlesinger, M. D., Demeter, J. J. and Greyson, M., "Catalyst for Producing Methane From H₂ and CO," I&EC Prod. Process Develop. 48, 68-70 (1956).
17. Schuster, V. F., Panning, G. and Bulow, H., "Methanation in Gas Mixtures Containing Carbon Monoxide and Carbon Dioxide With Various Nickel Catalysts," Brennst. Chem. 14, 306-07 (1935).
18. Strickland-Constable, R. F., "The Synthesis of Methane From Carbon Monoxide and Hydrogen on a Nickel Catalyst," Gas Research Board Communication GRB 46 London, 1949.

19. Vlasenko, V. M., Yuzefovich, G. E. and Rusov, M. T., "Hydrogenation of CO and CO₂ on Nickel Catalyst," Kinet. Kataliz 6, 938-41 (1965).
20. Vlasenko, V. M., Yuzefovich, G. E. and Rusov, M. T., "Kinetics of CO₂ Hydrogenation on a Nickel Catalyst," Kinet. Kataliz 2, 525-28 (1961).
21. Wainwright, H. W., Egleston, G. C. and Brock, C. M., "Laboratory-Scale Investigation of Catalytic Conversion of Synthesis Gas to Methane," Report No. 5046. Washington, D.C.: U.S. Dept. Interior, Bureau of Mines, 1954.
22. Yang, K. H. and Hougen, O. A., "Determination of Mechanism of Catalyzed Gaseous Reactions," Chem. Eng. Progr. 46, 146-57 (1950).

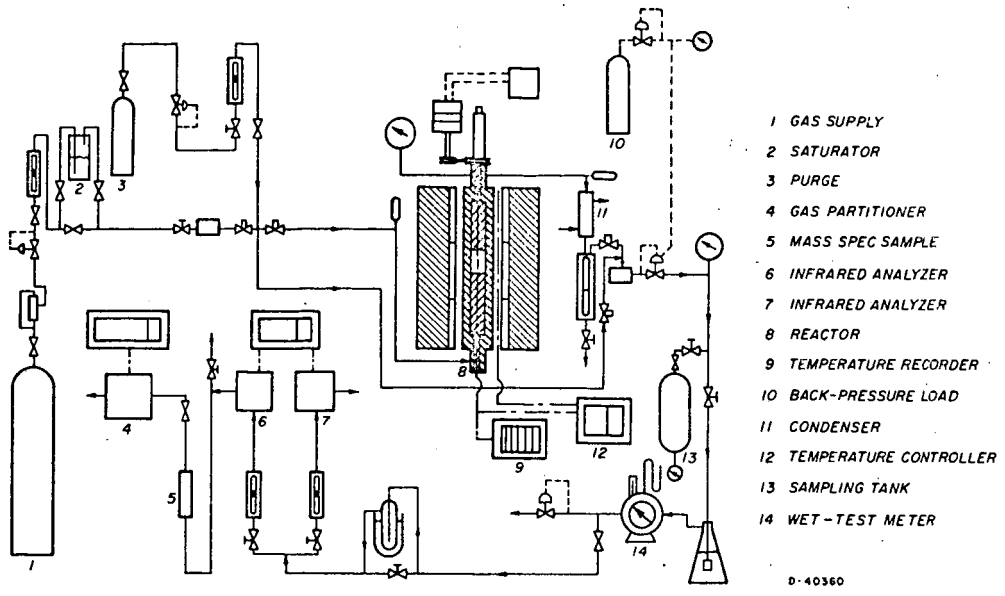


Figure 1. SCHEMATIC DIAGRAM OF METHANATION APPARATUS

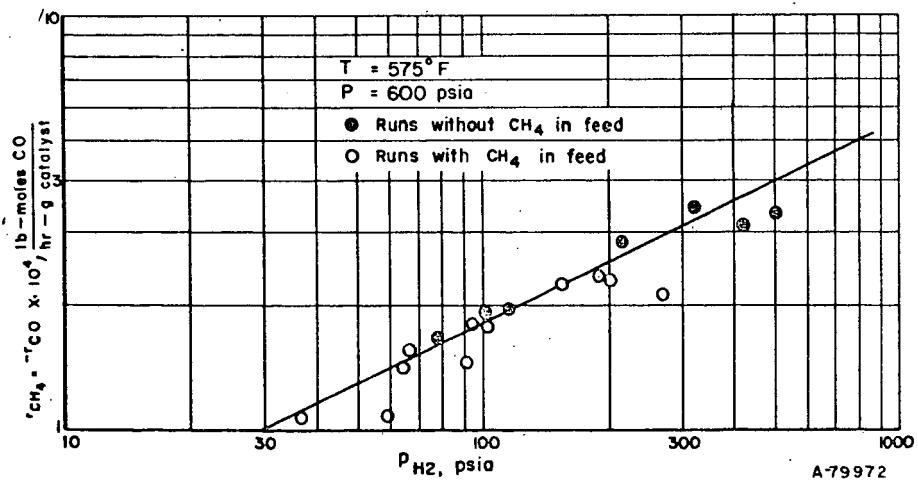


Figure 2. ORDER OF METHANATION REACTION WITH RESPECT TO HYDROGEN IS 1/2

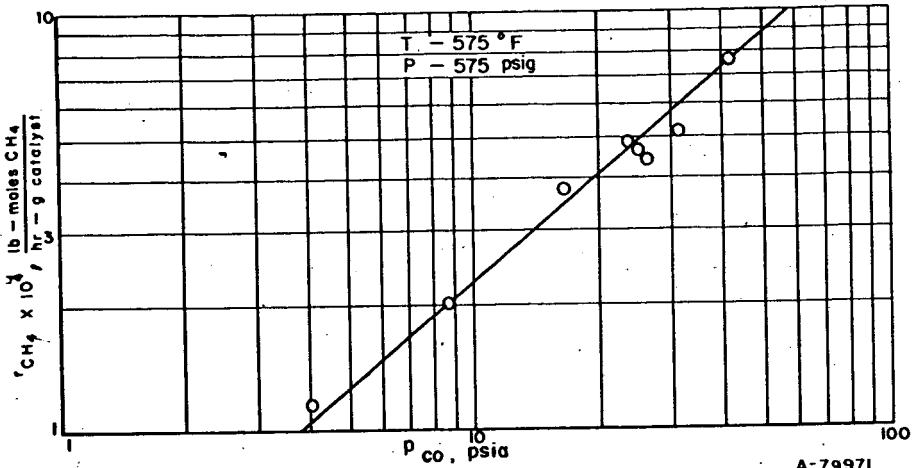


Figure 3. ORDER OF METHANATION REACTION WITH RESPECT TO CARBON IS 1

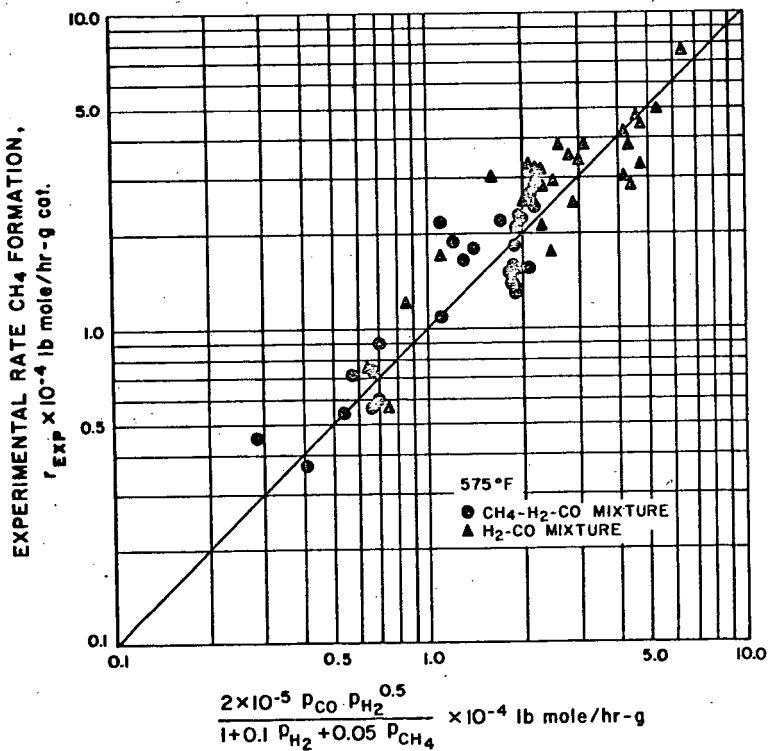


Figure 4. ANALYSIS OF METHANATION DATA

- LEGEND**
- A FEED-GAS STORAGE
 - B N₂ PURGE-GAS STORAGE
 - C FILTER
 - D PRESSURE GAGE
 - E PRESSURE REGULATOR
 - F ELECTRIC HEATER
 - G SULFUR REMOVAL
 - H ORIFICE
 - I DIFFERENTIAL PRESSURE TRANSMITTER
 - J FLOW RECORDING CONTROLLER
 - K SAFETY SHUTOFF
 - L DIFFERENTIAL PRESSURE GAGE
 - M ELECTRIC FURNACE
 - N METHANATION REACTOR
 - O CONDENSER
 - P DRAIN POT
 - Q STRIP CHART RECORDER
 - 1. TEMPERATURE
 - 2. COMPOSITION
 - R LEVEL CONTROLLER
 - S TEMPERATURE CONTROLLER
 - T ROTAMETER
 - U GAS DRIER
 - V INFRARED CO ANALYZER
 - W ZERO GAS
 - X CALIBRATION GAS
 - Y SATURATOR
 - Z WET-TEST METER

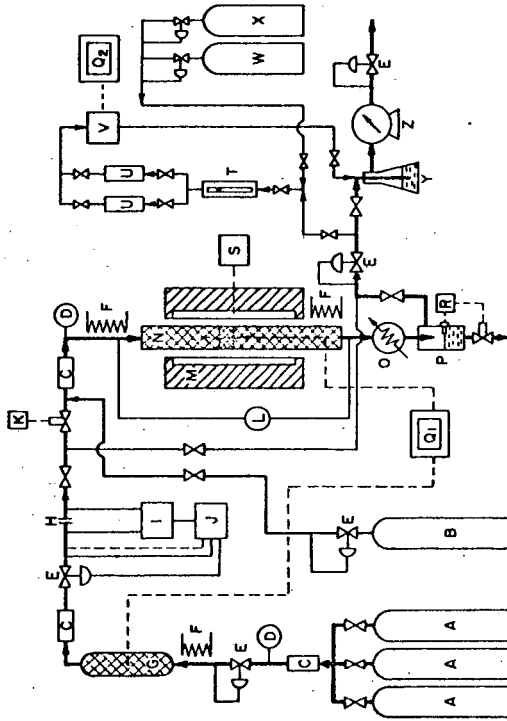


Figure 5. METHANATION LIFE-TEST UNIT

B-40334

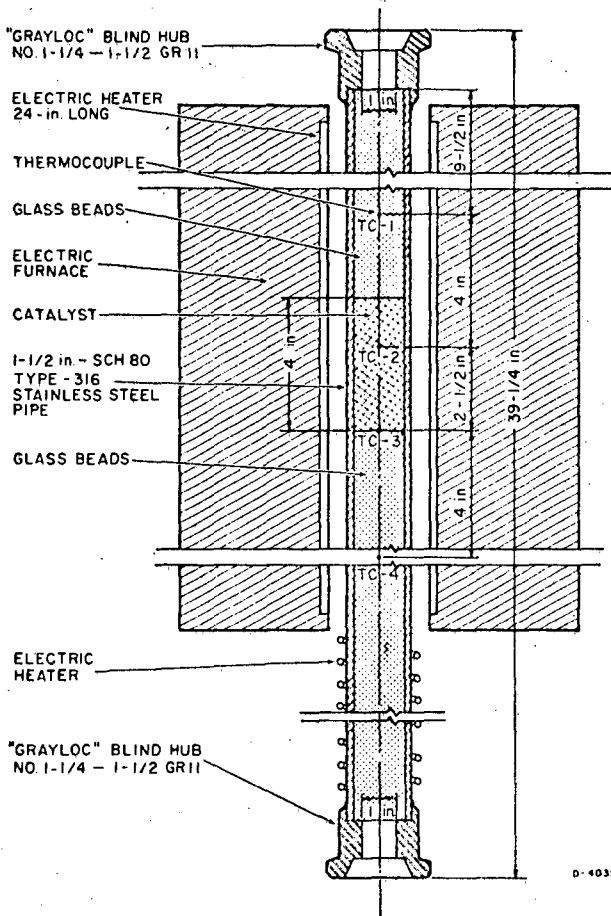


Figure 6. LABORATORY FIXED-BED REACTOR

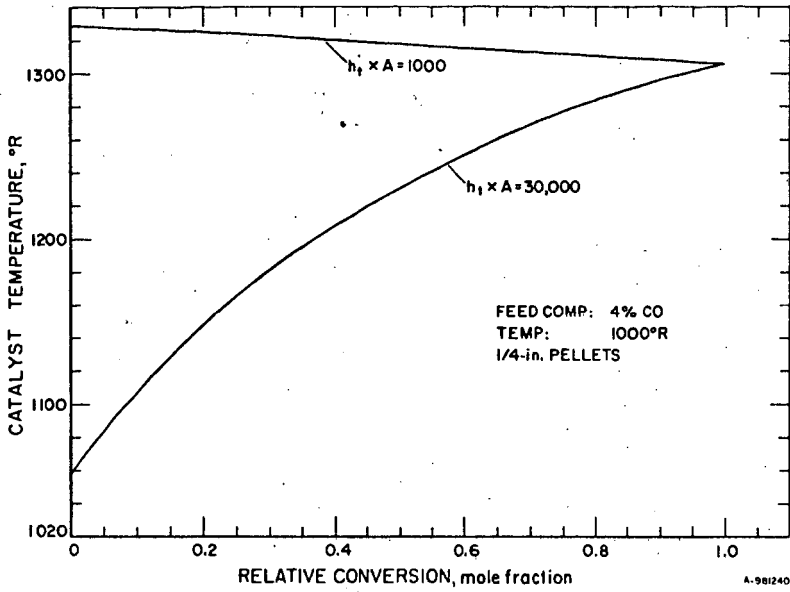


Figure 7. ESTIMATED STEADY-STATE TEMPERATURES IN METHANATION REACTOR

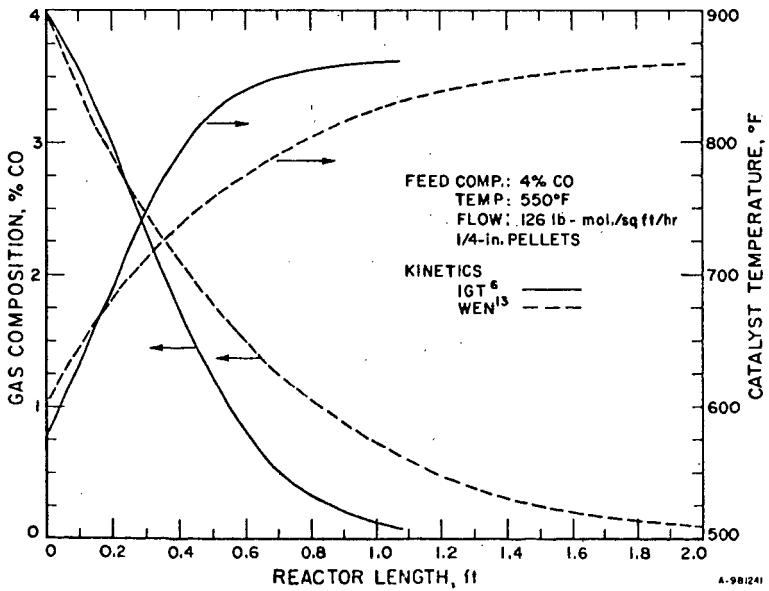


Figure 8. CALCULATED METHANATION REACTOR PERFORMANCE